Weatherill, G., Esposito, S., Iervolino, I., Franchin, P., Cavalieri, F. (2014) Framework for seismic hazard analysis of spatially distributed systems In: SYNER-G: Systemic Seismic Vulnerability and Risk Assessment of Complex Urban, Utility, Lifeline Systems and Critical Facilities, K. Pitilakis, P. Franchin, B. Khazai and H. Wenzel (eds.) ISBN 978-94-017-8834-2.

Chapter 3
Framework for Seismic Hazard Analysis of Spatially Distributed Systems

Graeme Weatherill, Simona Esposito, Iunio Iervolino, Paolo Franchin, and Francesco Cavalieri

Abstract The analysis of seismic risk to multiple systems of spatially distributed infrastructures presents new challenges in the characterisation of the seismic hazard input. For this purpose a general procedure entitled "Shakefield" is established, which allows for the generation of samples of ground motion fields for both single scenario events, and for stochastically generated sets of events needed for probabilistic seismic risk analysis. For a spatially distributed infrastructure of vulnerable elements, the spatial correlation of the ground motion fields for different measures of the ground motion intensity is incorporated into the simulation procedure. This is extended further to consider spatial cross-correlation between different measures of ground motion intensity. In addition to the characterisation of the seismic hazard from transient ground motion, the simulation procedure is extended to consider secondary geotechnical effects from earthquake shaking. Thus the Shakefield procedure can also characterise the effects site amplification and transient strain, and also provide estimates of permanent ground displacement due to liquefaction, slope displacement and coseismic fault rupture.

G. Weatherill (✉)
European Centre for Training & Research in Earthquake Engineering (EUCENTRE), Pavia, Italy
e-mail: graeme.weatherill@eucentre.it

S. Esposito • I. Iervolino
Dipartimento di Strutture per l'Ingegneria e l'Architettura, Università degli Studi di Napoli Federico II, Via Claudio 21, 80125 Naples, Italy

P. Franchin • F. Cavalieri
Department of Structural and Geotechnical Engineering, Sapienza University of Rome, Via Gramsci 53, 00197 Rome, Italy

K. Pitilakis et al. (eds.), *SYNER-G: Systemic Seismic Vulnerability and Risk Assessment of Complex Urban, Utility, Lifeline Systems and Critical Facilities*, Geotechnical, Geological and Earthquake Engineering 31, DOI 10.1007/978-94-017-8835-9_3,

3.1 Generating Seismic Scenarios for Spatially Distributed System Risk Analysis: An Overview of Concepts and Data Needs

3.1.1 Seismic Scenarios for Spatially Distributed System Analysis

The analysis of seismic risk to urban infrastructures within a region represents an important development in the effective mitigation of both economic and human losses due to earthquakes. To model the consequences of damage and failure to multiple interconnected systems it is important to define the seismic scenarios in a manner that is consistent with the properties of observed ground motions. The extension of seismic risk analysis to multiple systems of spatially distributed infrastructures presents new challenges in the characterisation of the seismic hazard input, particularly with respect to the spatial correlation structure of the ground motion values that form the basis for the systemic risk analysis.

An increasingly common approach for the estimation of losses for a spatially distributed portfolio of vulnerable elements is in the use of scenario events, or, if a probabilistic loss analysis is required, from a set of stochastically generated events that are representative of the earthquake recurrence models for the seismogenic sources under consideration. From these event sets it is possible to create realisations of ground motion fields, which are then input into the models of seismic risk.

3.1.2 Uncertainty and Spatial Correlation

For spatially distributed portfolios or systems, the spatial correlation structure of the ground motion fields may impact upon analyses of loss, and therefore cannot be neglected from the modelling process.[1] There is clear precedent in recent research into seismic risk, to take into account the spatial correlation between ground motions on an urban scale (Park et al. 2007; Crowley et al. 2008a,b; Goda and Hong 2008a,b; Jayaram and Baker 2010a).

When modelling seismic risk to urban infrastructure and complex interconnected systems, new challenges emerge in the process of generating the spatially correlated fields of ground motion. In the examples cited previously, the consideration of spatial correlation has been limited to fields of ground motion represented by a single ground motion intensity measure (IM), such as peak ground acceleration (PGA) or spectral acceleration ($S_a(T)$) or displacement ($S_d(T)$) at a specified period of oscillation (T). If considering multiple infrastructures, however, fragility

[1] Spatially distributed ground motion intensities are modelled as joint lognormal random fields herein; thus, correlation provides a complete description of their statistical structure.

models for different components of each infrastructure may require the characterisation of different measures of ground motion intensity, often depending on the physical properties (such as fundamental elastic period or, in the case of pipelines, the transient strain) of the element in question. Therefore in generating the ground motion fields, it may be inappropriate to characterise the spatial distribution of ground motion intensity using a single intensity measure, but instead the fields of many spatially correlated intensity measures may be required.

As the interconnection between infrastructural systems cannot be neglected, neither can the correlation between spatial fields of different intensity measures generated from the same event. Therefore, a critical challenge of this work is to extend process of generating fields of spatially correlated ground motion, to one in which the spatial cross-correlation structure is also represented.

The consideration of seismic risk to infrastructures introduces a further set of requirements in terms of seismic input. These relate to the geotechnical hazards associated with earthquakes, namely amplification and modulation of ground shaking at the Earth's surface due to the local site conditions (e.g., superficial geology, topography, deep geological structure etc.), and permanent ground displacement (PGD) arising due to liquefaction, slope displacement and co-seismic rupture around the fault surface. These hazards have a significant impact upon a many different infrastructures, particularly those with buried linear elements, which may traverse different geological formations within the interconnected system and are therefore vulnerable to permanent differential ground displacements. An assessment of risk to multiple systems of interconnected spatially distributed elements must therefore incorporate the geotechnical hazards in a manner that is also consistent with the ground shaking hazard.

3.1.3 The Shakefield Procedure

Initially, the focus of this analysis is upon generating fields of strong ground motion using earthquake scenarios. Each Shakefield represents a simulated strong ground motion field for a given rupture scenario. For a Shakefield, no recorded strong motion data are integrated into the strong motion fields that are generated. Shakefields can be adopted for single earthquake scenarios, a scenario in this context representing the source and magnitude of a single event, or can be applied within a probabilistic seismic hazard analysis, which considers many source and magnitude scenarios to effectively sample the variability in the seismogenic source. Each Shakefield is implemented in the following steps, and illustrated in Fig. 3.1:

1. Generate a source event with a given magnitude and source geometry. The geometry may take the form of a point or a finite rupture surface, the latter being preferred for consistency with the physical properties of the earthquake source. The source event may be a single scenario event (e.g. a historical earthquake or a hypothetical adverse case), or may be a sample from a probability distribution

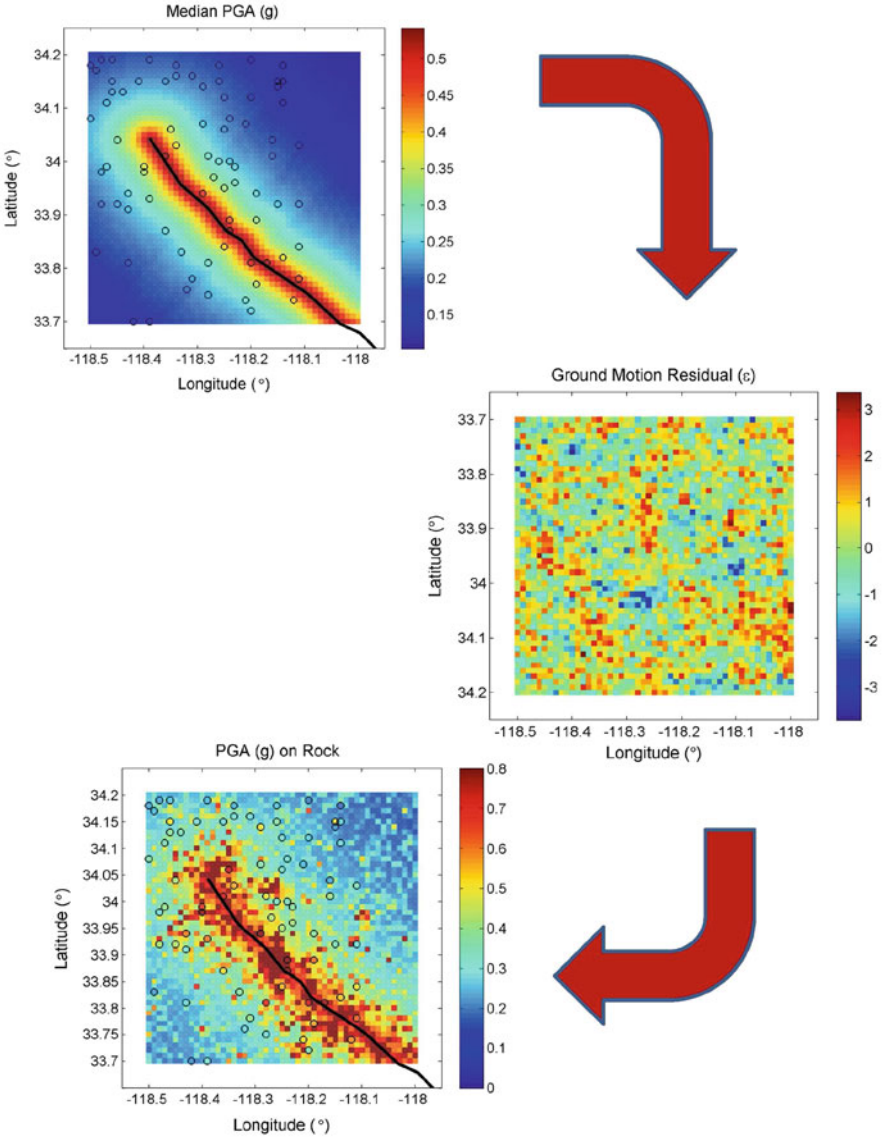

Fig. 3.1 Overview of the Shakefield process for strong motion on rock: attenuation of median ground motion (*top*), generation of field of spatially correlated ground motion residuals (*middle*) and calculation of ground motion on rock (*bottom*). Fault source indicated by *black line*, target sites indicated by *black circles*

representing the total magnitude frequency distribution of the seismogenic source and the set of potential seismogenic sources under consideration (see also Chap. 2).
2. Given a source and magnitude, and using a ground motion prediction equation (GMPE), attenuate the median ground motion field across spatial grid of locations considered in the system. Depending on the context and the number of locations under consideration, the nodes of the field may be the locations of the elements themselves, or a regularly spaced grid of points from which the ground motions at the element locations can be interpolated.
3. Generate a realisation of a standard Gaussian field representing the spatial correlation structure of a required intensity measure. For each site these variates are multiplied by the uncertainty terms of the GMPE and added to the median value on rock, thus sampling the ground motion uncertainty.
4. For each site, generate the ground motion values for the secondary intensity measures, conditional upon the simulated ground motion intensity measure of the primary IM.
5. Using an amplification factor appropriate to the soil conditions, and earthquake intensity, at each site, scale the ground motions to give the ground motion field on soil.
6. If required, proceed to define a geotechnical hazard parameter (e.g. permanent ground deformation resulting from liquefaction or slope displacement) conditional upon the intensity of ground motion at the site.

Given the scenario event, it is necessary to determine the rupture geometry. The complexity of the rupture model, and the degree of detail resolved, may depend strongly on the amount of information available to define the seismogenic source. This may, in simplest cases, define the rupture as simply a point or line source from which energy radiates in an isotropic manner. In most applications, however, the seismic source may be defined as a simple geometric rupture plane in three dimensions. This may correspond to a fault segment, or partial segment, or may be an approximation to the rupture plane of a previous event. Simple geometrical approximations to the rupture surface may be useful in hazard-based approaches where aleatory variability arising from different rupture scenarios may be constrained to the selected fault plane, without requiring a priori assumptions about the rupture dynamics.

After defining the scenario rupture, the ground motion can be attenuated from the source. Again, several methods may be employed at this point, some of which may be more appropriate than others given the limitations of the available fault rupture model. Numerical simulations of ground motion attenuation may naturally extend from those of the rupture model. These methods are reliant on detailed geological and geotechnical models of the medium through which the waves travel and of the site conditions. For site-specific analysis such detailed models may be feasible to determine. On a larger scale, including that of a city, the accuracy of the geological models may be harder to constrain at the resolution needed for numerical analysis.

For seismic sources defined according to a simple rupture geometry, the most common method of generating a Shakefield is via the use of GMPEs. A typical ground motion model is derived from observed strong motion records, with parameters fitted by regression between the intensity measure of interest and the source and site characteristics:

$$\log\left(Y_{ij}\right) = \overline{\log Y_{ij}}\left(M_i, R_{ij}, \theta_{i1,i2,\ldots,iN}\right) + \tau\eta_i + \sigma\epsilon_{ij} \tag{3.1}$$

where Y_{ij} is the ground motion intensity measure at site j during the earthquake i, and $\overline{\log Y_{ij}}$ the mean of the logarithms of the IM, at distance R_{ij} from earthquake with magnitude M_i. $\theta_{i1,i2,\ldots,iN}$ are additional parameters that may describe characteristics of the site or earthquake source. Uncertainty in the ground motion is separated into an inter-event $\tau\eta_i$ and intra-event $\sigma\epsilon_{ij}$ residual term, where η_i and ϵ_{ij} are normally distributed random variables with means of zero and standard deviations of unity, and τ and σ are the standard deviations of the inter- and intra-event terms.

3.2 Empirical Modelling of Ground Motion Spatial Correlation and Spectral Correlation

The Shakefield process is intended to provide the ground motion input for the fragility models of the vulnerable elements of each infrastructure in a complex interconnected system of infrastructures, such as a city comprising a building stock and multiple lifeline networks. As the systems themselves, and the elements within, are connected, it is critical that spatial correlation is incorporated into the simulation process. The simulation of the spatially correlated fields of ground motion, presented in detail in Sect. 3.3, requires the use of empirically derived models of correlation between intensity measures and also across spatial domains within each intensity measure. These models are typically derived from databases of observed ground motion records, or in the case of spatial correlation models from strong motion records from individual events. In this section existing models of intensity measure intra-event residuals correlation (Sect. 3.2.1) and spatial correlation (Sect. 3.2.2) are summarised, and the spatial correlation models of Esposito and Iervolino (2011, 2012) presented, which are derived from European records.

3.2.1 Correlation Between Intensity Measures Recorded at the Same Site

From the definition of an empirical ground motion intensity model given in Eq. 3.1, correlations between ground motion intensity measures pertain to the residual term

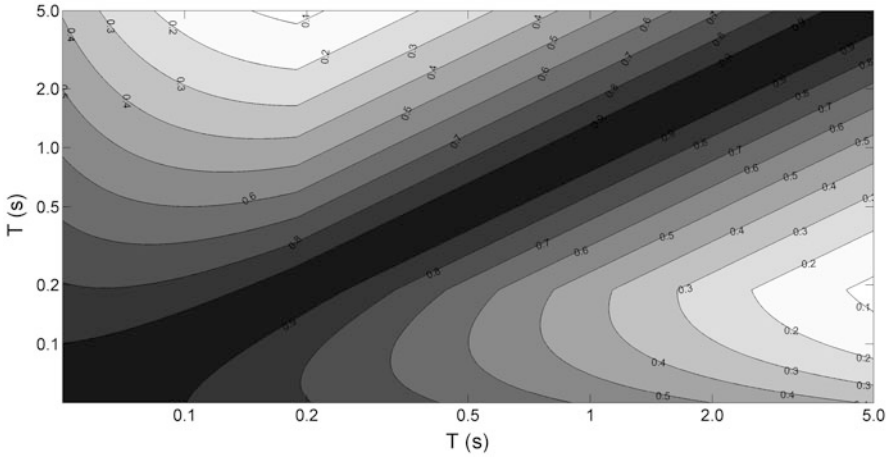

Fig. 3.2 Coefficient of correlation in the GMPE residual between spectral accelerations for two different periods of motion (T_1 and T_2) recorded at the same site, according to the model of Baker and Cornell (2006) given in Eq. 3.2

$\varepsilon_{ij}\sigma_T$, where $\sigma_T = \sqrt{\tau^2 + \sigma^2}$. Several models have been proposed in previous literature for correlation of pseudo-spectral accelerations recorded at the same site (Inoue and Cornell 1990; Baker and Cornell 2006; Baker and Jayaram 2008). The spectral acceleration correlation model of Baker and Cornell (2006) is preferred in the current analysis, shown here and in Fig. 3.2:

$$\rho_{\varepsilon_x,\varepsilon_y} = 1 - \cos\left(\frac{\pi}{2} - \left(0.359 + 0.163 I_{(T_{min}<0.189)} \ln\frac{T_{max}}{T_{min}}\right)\ln\frac{T_{max}}{T_{min}}\right) \quad (3.2)$$

where $\rho_{\varepsilon_x,\varepsilon_y}$ is the coefficient of correlation of the ground motion residual term between spectral acceleration between two periods $S_a(T_1)$ and $S_a(T_2)$ for two different horizontal components of motion recorded at the same site, $T_{max} = \max[T_1, T_2]$ and $T_{min} = \min[T_1, T_2]$ and I takes the value of 1 if $T_{min} < 0.189$ and 0 otherwise. This model is preferred here for application in Europe over the model of Baker and Jayaram (2008), in part due to the selection of the Akkar and Bommer (2010) GMPE, which uses the ordinary geometric mean of the horizontal components of ground motion, as opposed to the models from which the Baker and Jayaram (2008) model is derived, which themselves use the rotationally independent geometric mean.

The IM correlation models do not extend only to spectral accelerations. Baker (2007) presents a similar model to describe the correlation between Arias Intensity (I_a) and spectral acceleration, whilst Bradley (2011a,b) computes the correlation between spectral acceleration and other ground motions intensity measures such as duration, acceleration spectrum intensity and velocity spectrum intensity.

3.2.2 Spatial Correlation Models in Ground Motions

Correlation of ground motion intensity measures in a single earthquake is due to the parameters that appear in the GMPEs, such as the magnitude, and spatial correlation of the intra-event residuals ϵ_{ij}. The multivariate Gaussian distribution has been found suitable (Jayaram and Baker 2008) to model a single intensity measure across multiple sites. Many analyses of spatial correlation are limited to a few earthquakes for which there exists a dense network or strong motion records. The scarcity of densely recorded events, particularly in Europe, requires that empirical models be derived from databases of ground motion record, combining data from different earthquakes.

3.2.2.1 Empirical Models of Spatial Correlation from European Strong Motion Records

Spatial correlation models of intra-event residuals available in literature have been mostly estimated using single non-European earthquakes (e.g., Northridge 1994, Japanese earthquakes occurred from 2000 to 2003, Chi-Chi 1999), for which many records were available from dense seismic networks (e.g. Boore et al. 2003; Wang and Takada 2005; Goda and Hong 2008a; Jayaram and Baker 2009). Those models depend on inter-site separation distance (h) and provide the limit at which correlation may technically considered to be lost (i.e., distance beyond which intra-event residuals of IMs at different sites may be considered uncorrelated).

The different decay rates of spatial correlation models available in literature could depend on choices made in the estimation or on the GMPE used; moreover there could be a dependency related to the particular region or earthquake characteristics. The estimation of an appropriate spatial correlation model requires several tasks be undertaken, each with associated possible options: (i) choice of dataset to obtain the intra-event residuals: this means choosing which and how many records to consider (single or multiple earthquakes); (ii) choice of GMPE to obtain residuals e.g. from existing GMPEs or ad hoc attenuation laws (i.e., estimated on the chosen dataset); (iii) working assumptions of the estimation.

For example, Sokolov et al. (2010), starting from the strong-motion database of Taiwan Strong Motion Instrumentation Program (TSMIP) network, estimated correlation for various areas, site classes, and geological structures, asserting that a single generalized spatial model may not be adequate for all of Taiwan territory. Conversely, Goda and Atkinson (2009) also investigated the effects of earthquake types on correlation parameters using datasets from K-NET and KiK-net Japanese strong-motion networks without finding any significant dependency. In some cases (e.g. Wang and Takada 2005; Jayaram and Baker 2009), existing GMPEs are used, while in others (e.g. Goda and Hong 2008a; Goda and Atkinson 2009; Sokolov et al. 2010), an ad hoc fit on the chosen dataset is adopted. Generally, regression analysis used to develop prediction equations does not incorporate the correlation

structure of residuals as a hypothesis. Hong et al. (2009) and Jayaram and Baker (2010b) evaluated the influence of considering the correlation in fitting a GMPE, finding a minor influence on regression coefficients and a more significant effect on the variance components. Goda and Atkinson (2010) investigated the influence of the estimation approach, emphasising its importance when residuals are strongly correlated.

The joint distribution of the logs of the IMs at all locations of interest that are assumed to be values of Gaussian random field (GRF), have a covariance matrix that is characterised, in the simplest of these spatial correlation models, by one parameter: the *range*. This parameter represents the inter-site distance at which the spatial correlation is practically lost.

In the European strong motion datasets, no dense observations of single earthquakes are available from which reliable estimates of spatial correlation of intensity measures can be obtained. Therefore, an ensemble of strong motion records from multiple events and regions was used to obtain a unique model (Esposito and Iervolino 2011, 2012) using the European Strong-motion Database (ESD) and the Italian Accelerometric Archive (ITACA). The GMPEs with respect to which residuals were computed were those of Akkar and Bommer (2010) for ESD, and Bindi et al. (2010b, 2011) for ITACA. Subsets of the same records used to estimate the considered GMPEs were used to perform intra-event spatial correlation models.

The analysis of correlation was performed for different IMs (i.e. PGA, PGV and spectral acceleration, $S_a(T)$) via the use of geostatistical tools. In particular, the semivariogram, $\gamma(h)$, was used to model the covariance structure of the different IMs through mathematically tractable functions fitted to empirical observations.

In building a unique semivariogram from multiple events, individual events were first treated separately, before aggregating all the possible distance pairs into a single experimental data set. An empirical trend was fitted to the data assuming an exponential model as expressed here:

$$\gamma(h) = 1 - e^{-3h/b} \tag{3.3}$$

The resulting *range (b)* was found to be 13.5 km (ESD) and 11.5 km (ITACA) for PGA and 21.5 km (ESD) and 14.5 km (ITACA) for PGV (Esposito and Iervolino 2011).

For $S_a(T)$ (5 % damped) residuals the evaluation of the spatial correlation was carried out at seven structural periods, ranging from 0.1 to 2 s, for the Italian dataset, and 0.1–2.85 s (nine periods) for the European dataset. The results are summarised in Table 3.1. Correlation length (b) tends to increase with period as also confirmed by other studies (Jayaram and Baker 2009).

Finally, in order to capture the trend of the range as a function of structural period T, for each dataset a linear-predictive model was fitted as expressed by:

$$b(T) = d_1 + d_2\, T \tag{3.4}$$

Table 3.1 Estimated ranges for spectral acceleration residuals using the Akkar and Bommer (2010) and Bindi et al. (2011) GMPEs (Esposito and Iervolino 2012)

GMPE	Period (s)	b (km)	GMPE	Period [s]	b [km]
	0.1	13.7		0.1	11.4
	0.2	11.6		0.2	9.0
	0.3	15.3		0.3	13.2
Akkar and Bommer (2010)	0.5	12.5	Bindi et al. (2011)	0.5	11.9
	1.0	33.9		1.0	17.8
	1.5	27.0		1.5	25.7
	2.0	39.0		2.0	33.7
	2.5	40.5			
	2.85	48.8			

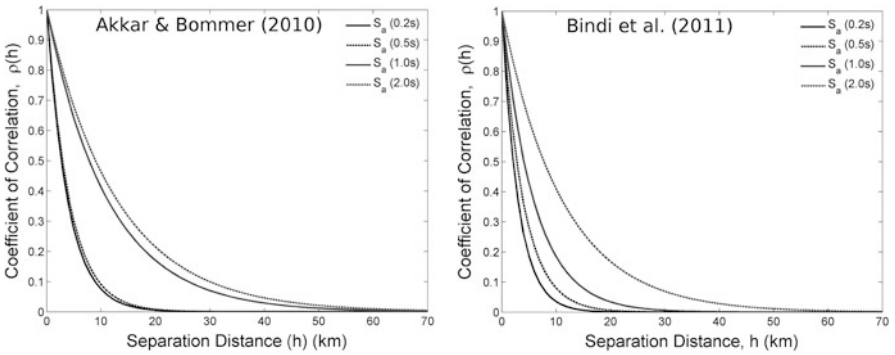

Fig. 3.3 Coefficient of spatial correlation for selected spectral periods derived using the Akkar and Bommer (2010) (*left*) and Bindi et al. (2011) (*right*) GMPEs from the correlation models of Esposito and Iervolino (2012)

where models parameters d_1 and d_2 are found to be 11.7 and 12.7, respectively, for the ESD dataset and 8.6 and 11.6, respectively, for the ITACA dataset. Comparisons of the spatial correlation models for the different periods are seen in Fig. 3.3.

3.3 Simulation of Spatially Correlated and Spatially Cross-Correlated Ground Motion Fields

The stochastic simulation of spatially correlated fields is a challenging task that has many applications in various fields of engineering and geosciences. Different methods are available to implement this approach, of which the simplest is the Matrix Decomposition method (Davis 1987). The problem is approached only in two dimensions (i.e. only considering the distribution of intra-event residuals at the

surface) for convenience and efficiency. Whilst there may be merit in describing the simulation of ground motion at depths below the surface, the paucity of strong motion borehole data limits the extent to which the correlation between ground motion at different depths can be characterised. It is assumed that where subterranean lifeline elements such as gas, oil or water pipelines are considered, they are at sufficiently shallow depths as to be adequately modelled via analysis of surface ground motion. In the cases of spatially distributed subterranean systems it may be more appropriate to model vulnerability by numerical simulation of ground motion across a 3D mesh. Full constraint of the geological properties of the environment requires detailed investigation, which may only be considered follow in special circumstances.

There are many different techniques available for generating random fields with given correlation properties. It is to be expected that the manner in which multiple intensity measures are generated across a spatially distribute system will have a non-negligible impact on the resulting analyses of system performance. Two possible methods are presented and appraised here on the basis of their underlying assumptions and the challenges when applying them to real urban infrastructure analyses.

3.3.1 Conditional Simulation

The process of conditional simulation represents, in effect, a stochastic sampling of the joint probability distribution function of two correlated variables. The variables are assumed to be distributed according to a bivariate Gaussian distribution. For two given IMs (IM_1 and IM_2), each assumed to be lognormally distributed with a mean ($\mu_{\log IM_1}$ and $\mu_{\log IM_2}$) and variance ($\sigma_{\log IM_1}$ and $\sigma_{\log IM_2}$) and correlation coefficient $\rho_{\log IM_1, \log IM_2}$, the conditional distribution of IM_2 upon the value (z) generated for IM_1, given a magnitude M and source to site distance R, is described by Iervolino et al. (2010):

$$\mu_{\log IM_2 | \log IM_1, M, R} = \mu_{\log IM_2 | M, R} + \rho_{\log IM_1, \log IM_2} \sigma_{\log IM_2} \frac{z - \mu_{\log IM_1, M, R}}{\sigma_{T \log IM_1}} \quad (3.5)$$

$$\sigma_{T \log IM_2 | \log IM_1} = \sigma_{T \log IM_2} \sqrt{1 - \rho^2_{\log IM_1, \log IM_2}} \quad (3.6)$$

Note that these equations refers to the case in which the GMPE does not distinguish between inter-event and intra-event residuals, yet the method is readily applicable also in such a case.

The simulation of IM_1 and IM_2 is implemented via the following procedure:

Algorithm 3.1 Description of co-simulation via the sequential simulation process, conditional upon on a primary intensity measure

Data: Primary IM selection, Spatial correlation model, IM-correlation model, event source, magnitude, GMPE
Result: Ground Motion Fields for each IM
for $i \leftarrow 1$ **to** $N_{Earthquakes}$ **do**
  Generate Source
  Calculate Median Ground Motion at Sites for Primary IM $\mu_{\log IM_1 \mid M,R}$
  Generate Spatially Correlated Field of Ground Motion Residuals
  Multiply residuals by standard deviation of Primary IM σ_{IM_1}
  for $IM_j \in SecondaryIMs$ **do**
    Calculate Median Ground Motion Field at Sites $\mu_{IM_j \mid M,R}$
    Calculate the conditional mean ($\mu_{\log IM_j \mid \log IM_1,M,R}$) and standard deviation ($\sigma_{\log IM_j \mid \log IM_1}$ of IM_j) using (3.5) and (3.6)
    Sample IM_2 from a Gaussian distribution with a mean and standard deviation of $\mu_{\log IM_j \mid \log IM_1,M,R}$ and $\sigma_{\log IM_j \mid \log IM_1}$ respectively.
  end
end

This approach has several practical advantages that make it suitable for application here. The LU decomposition need only be performed once for the primary IM at the initiation of the simulation, and only one spatially correlated field generated per event. For application to multi-system infrastructures, this is particularly advantageous as it permits for the generation of secondary IMs at sites only where required by the fragility model of the system element at a particular site.

The second advantage is that the sequential approach avoids making explicit assumptions about the nature of the cross-correlation structure between two IM fields. Instead the spatial simulation can be conditioned upon the IM for which the spatial correlation model is best constrained.

The formulation of the conditional approach requires the assumption that the ground motion field of a secondary IM is conditional only upon the primary IM at the same site, and conditionally independent of all else. If this is the case, the spatial correlation structure of the secondary IM is respected in this approach. In practice, however, this may be a strong assumption, which should be verified before applying the conditional simulation approach.

3.3.2 Extended Matrix Decomposition

This approach is an extension to two fields of the LU decomposition presented previously for simulation of a single field. A Gaussian random field can be defined as:

$$\mathbf{Y_1} = \boldsymbol{\mu}_{\mathbf{log}}\mathbf{IM_1} + \mathbf{L_1}\mathbf{Z_1} \tag{3.7}$$

where $\boldsymbol{\mu}_{\mathbf{log}}\mathbf{IM_1}$ is the mean of the field (assumed here to be zero-vector for the ground motion residuals), $\mathbf{Z_1}$ is a vector of independently Gaussian distributed random variables and $\mathbf{L_1}$ is the root of the positive-definite covariance matrix ($\mathbf{C_{11}}$) such that $\mathbf{L_1 L_1^T} = \mathbf{C_{11}}$ (e.g. Park et al. 2007; Crowley et al. 2008a).

Consider then a second field ($\mathbf{Y_2}$), with mean $\boldsymbol{\mu}_{\mathbf{log}}\mathbf{IM_2}$ and covariance matrix $\mathbf{C_{22}}$, for which the correlation between a common two elements in $\mathbf{Y_1}$ and $\mathbf{Y_2}$ separated by a distance (h) of 0 km is given by $\rho_{\log IM_1, \log IM_2}$ ($\rho_{1,2}$ hereafter) the following model is generated (Oliver 2003):

$$\begin{bmatrix} \mathbf{Y_1} \\ \mathbf{Y_2} \end{bmatrix} = \begin{bmatrix} \boldsymbol{\mu}_{\mathbf{log}}\mathbf{IM_1} \\ \boldsymbol{\mu}_{\mathbf{log}}\mathbf{IM_2} \end{bmatrix} + \begin{bmatrix} \mathbf{L_1} & \mathbf{0} \\ \rho_{1,2}\mathbf{L_2} & \sqrt{1-\rho_{1,2}^2}\mathbf{L_2} \end{bmatrix} \begin{bmatrix} \mathbf{Z_1} \\ \mathbf{Z_2} \end{bmatrix} \tag{3.8}$$

where Z_2 is a vector of independently Gaussian distributed random variables and $\rho_{1,2}$ the cross-covariance between fields Y_1 and Y_2. The total cross-covariance matrix $\mathbf{L}$ is therefore described by:

$$\mathbf{L}\mathbf{L}^{\mathbf{T}} = \begin{bmatrix} \mathbf{L_1 L_1^T} & \rho_{1,2}\mathbf{L_1 L_2^T} \\ \rho_{1,2}\mathbf{L_2 L_1^T} & \mathbf{L_2 L_2^T} \end{bmatrix} \tag{3.9}$$

This formulation can be expanded further to consider multiple IMs, with the full cross-covariance matrix given by:

$$\mathbf{L}\mathbf{L}^{\mathbf{T}} = \begin{bmatrix} \mathbf{L_1 L_1^T} & \rho_{1,2}\mathbf{L_1 L_2^T} & \cdots & \rho_{1,j}\mathbf{L_1 L_j^T} \\ \rho_{2,1}\mathbf{L_2 L_1^T} & \mathbf{L_2 L_2^T} & \cdots & \rho_{2,j}\mathbf{L_2, L_j^T} \\ \vdots & \vdots & \ddots & \vdots \\ \rho_{i,1}\mathbf{L_i L_1^T} & \rho_{i,2}\mathbf{L_i L_2^T} & \cdots & \mathbf{L_i L_i^T} \end{bmatrix} \tag{3.10}$$

which within the simulation becomes:

$$\begin{bmatrix} \mathbf{Y_1} \\ \mathbf{Y_2} \\ \vdots \\ \mathbf{Y_i} \end{bmatrix} = \begin{bmatrix} \boldsymbol{\mu}_{\mathbf{log}}\mathbf{IM_1} \\ \boldsymbol{\mu}_{\mathbf{log}}\mathbf{IM_2} \\ \vdots \\ \boldsymbol{\mu}_{\mathbf{log}}\mathbf{IM_i} \end{bmatrix} + \mathbf{L} \begin{bmatrix} \mathbf{Z_1} \\ \mathbf{Z_2} \\ \vdots \\ \mathbf{Z_i} \end{bmatrix} \tag{3.11}$$

where $\mathbf{L}$ is determined from Cholesky factorization of the full block cross-correlation matrix $\mathbf{L}\mathbf{L}^{\mathbf{T}}$. Assuming the covariance structure of each of the fields ($\mathbf{C_{ii}}$) is real-valued and positive-definite, $\mathbf{L}$ will be real. If the correlation between the strong motion residuals is assumed to be isotropic, an assumption largely supported by the analysis of Jayaram and Baker (2009), then C_{ii} will be positive-definite. An example of three spatially cross-correlated, unconditional random fields of strong ground motion residuals is shown in Fig. 3.4.

In this method there is no requirement to assign a primary IM or secondary IM. As a means of defining the spatial cross-correlation for multiple fields, this method

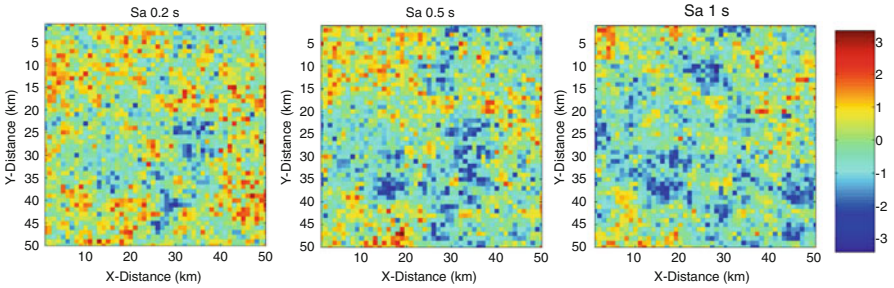

Fig. 3.4 Unconditional random co-simulation of strong ground motion residuals using the extended LU decomposition method, for spectral accelerations at 0.2, 0.5 and 1.0 s respectively

shares many advantages with that of the linear model of co-regionalisation (LMCR) approach adopted by Loth and Baker (2013). Both are able to define the full cross-covariance matrix, and can be implemented similarly. The primary difference is that the latter is derived directly from the empirical cross-correlograms, whereas the former can utilise separate models for the spatial correlation and cross-correlation.

In implementation of the co-simulation methodology there are certain costs associated with this approach. Mostly these relate to the computational inefficiencies of the methodology. The full cross-correlation matrix must be constructed and factorised, which, if considering a large number of locations and/or IMs, requires considerable computation and memory allocation.

The choice of whether to adopt a conditional simulation or a full cross-correlation methodology will inevitably depend on the circumstances of the application. Primarily, whether the assumptions required by the conditional approach can be assumed. The impact and limitations of each methodology upon seismic risk analysis for multi-system infrastructures is an area that requires considerably more analysis and experimentation.

3.4 Stochastic Modelling of Geotechnical Hazards: Site Amplification and Permanent Ground Deformation (PGD)

Fragility models for many linear lifeline systems (e.g. roads, pipelines, rail tracks, underground electricity lines, oil, gas, water and waste water) will often require the input of the permanent ground deformation (PGD), in addition to the transient shaking. It is therefore imperative that when simulating the Shakefields the influence of the local geology is taken into consideration.

The characterisation of surficial geology and its influence on both the transient and permanent ground motion across a region of the scale of a large metropolitan area brings with it significant practical limitations. The selection of models relating

the surface ground displacement to the seismic hazard input must take into consideration the fact that, for much of a region, many properties of the geology are either not known, or must be conditioned upon a set of observations within the region. Therefore the reduction in variability in the model of site amplification and/or permanent displacement that accompanies a well-constrained geotechnical profile is offset by the paucity of observation points with respect to the number of sites considered in the analysis. It is within this context that a parsimony-driven approach is favoured here. A strong emphasis is placed on selecting practical methodologies for implementing site amplification and geotechnical hazard analysis across an urban region, and empirical models requiring complex characterisation of the soil profile may not necessarily be appropriate.

The need for practical implementation of a geotechnical hazard analysis across a wide spatial scale is, to a certain extent, addressed within the HAZUS (NIBS 2004) methodology. It has therefore been considered appropriate to retain specific elements of this process, such as the landsliding and liquefaction susceptibility classifications, and, in certain cases, the permanent ground displacement models where alternative formulations were not available. There is an important distinction, however, between the HAZUS methodology and the implementation here, and that is in the adoption of the stochastic framework for seismic hazard inputs. This allows us to utilise both the probability definitions (e.g. probability of slope failure given an acceleration greater than the yield acceleration of a site) and the variability of the empirical displacement models, directly within the simulation procedure. Therefore with each stochastically generated Shakefield an additional field of permanent ground displacements can be produced.

3.4.1 Site Amplification

The site amplification factor $AF(T)$, which describes the ratio of the spectral acceleration of ground motion at the ground surface $S_a(T)_{SURFACE}$ with to that of the ground motion in the engineering bedrock $S_a(T)_{ROCK}$ is defined according to (e.g. Bazzurro and Cornell 2004b):

$$AF(T) = \frac{S_a(T)_{SURFACE}}{S_a(T)_{ROCK}} \tag{3.12}$$

$$\ln S_a(T)_{SURFACE} = \ln S_a(T)_{ROCK} + \overline{\ln AF(T)} + \sigma_{T\ln AF(T)} \tag{3.13}$$

where $\overline{\ln AF(T)}$ represents the median amplification factor and $\sigma_{T\ln AF(T)}$ its corresponding total uncertainty. For practical application the bedrock is assumed to correspond to Eurocode 8 (EC8) Type A soil. Several different estimators of $AF(T)$ may be implemented. The selection of the appropriate method is dependent on the case study, but for the present purpose it is assumed that the input microzonation

should provide sufficient information to define a Eurocode 8 site classification for each site at which the ground motion is required.

3.4.1.1 Direct Incorporation of GMPE Site Amplification Factors

Arguably the simplest approach is to utilise the site amplifcation models directly within the GMPE itself, simply by inputting the site class and/or V_{s30} value for each site in the ground motion field. For Akkar and Bommer (2010) or Bindi et al. (2010a) this requires the site class is input according to the NEHRP classifications (for NEHRP classes B, C and D only), whilst for other GMPEs it may be necessary to specify the V_{s30} directly (or use an assumed value on the basis of the site class). This approach is also the most consistent with the ground motion variability definition, as the uncertainty in the ground motion is defined given that the site parameter is known. However, the range of soil conditions for which the selected GMPEs are valid may be limited compared to the soil conditions observed in the study region. This is likely to be the case for regions with particularly soft or liquefiable soils. Few GMPEs can be applied to sites with V_{s30} less than 150 m s^{-1}, which would limit the validity of such GMPEs in harbour areas or for very soft alluvial beds.

An alternative approach would be to use an empirical amplification model such as that proposed by Choi and Stewart (2005):

$$\ln\left(AF_{ij}\right) = c\ln\left(\frac{V_{s30_{i,j}}}{V_{ref}}\right) + b\left(\frac{PHA_{r_{ij}}}{0.1}\right) + \tau_{\ln AF}\eta_i + \sigma_{\ln AF}\epsilon_{ij} \tag{3.14}$$

where $PHA_{r_{ij}}$ is the peak horizontal acceleration on rock at site j from earthquake i, and c, b and V_{ref} are constants, as defined in Choi and Stewart (2005). This model, derived from 1828 observed strong ground motions originating from 154 active shallow crustal earthquakes, describes the amplification as a continuum taking into account soil nonlinearity. The variability in the amplification function is separated into an inter- and intra-event term, $\tau_{\ln AF}\eta_i$ and $\sigma_{\ln AF}\epsilon_{ij}$ respectively. As with the GMPEs it may be limited to a narrow range of site conditions than is required for the case study in question.

3.4.1.2 Fixed Amplification Factors from Seismic Design Codes

In certain applications amplification of PGA, spectral acceleration or spectral displacements can be estimated using factors specified in appropriate design codes. For application within Europe, the amplification factors specified within Eurocode 8, and in more recent revisions (Pitilakis et al. 2012, 2013), are supported by the current methodology, as too are the amplification factors specified in the 1997 NEHRP Provisions (FEMA-450 2003), which form the basis for the amplification factors used by HAZUS.

As with the GMPE-based approach, this method has several advantages in terms of simplicity, and relatively minimal requirements in terms of the site classification. It is simple to implement across a region, with the advantage that the hazard itself must be specified only for the reference rock. This means there is little additional computational cost if it is necessary to interpolate between sites. Furthermore, the issue of linear or nonlinear amplification need not be addressed directly, as nonlinearity may be implicit in the code amplification factors.

By implementing code-based amplification factors, this approach is limited to site categories for which the code supplies such factors, and by the conservatism often implied by codes. An additional limitation is that design codes are unlikely to provide amplification factors for IMs other than PGA or spectral acceleration. Parameters such as Arias Intensity and Cumulative Absolute Velocity (CSV) have little use for structural design, even if they may be demonstrated to be relatively efficient predictors of damage or loss. This limits the extension of the code-based site amplification approach to less common IMs.

3.4.1.3 "Application-Specific" Amplification Factors

It may be the case that extensive microzonation studies have been undertaken for the region of application. The ability to integrate detailed microzonation information into the hazard analysis is an important means of reconciling the more general seismic hazard approach with the site-specific engineering approach to earthquake loss studies. For this purpose, it may be prudent to define amplifications factors, of the form described in Eq. 3.13, which are not necessarily generic or characteristic for a particular site class, but are specific to the sites for the application in question. They should be based on a higher level of geotechnical information than for the design code or GMPE approaches described previously, and should begin to incorporate information relevant to the structure of the subsurface and the dynamic properties of the material.

For each micro-zone within a given region, a characteristic site profile or set of profiles may be determined, possibly from borehole profiles or from non-invasive geophysical investigation. From this profile, and using a 1D numerical amplification tool, it is possible to estimate an amplification factor (AF_{ij}) particular to the micro-zone according to the formulation of Bazzurro and Cornell (2004a,b). Variability in the amplification factor may be attributed to record-to-record variation, and also to uncertainty in the site profile (e.g., Robinson et al. 2006). Bazzurro and Cornell (2004b) illustrate how this formulation can be combined with the hazard integral to allow for calculation of $S_a\,(T)_{SURFACE}$ for a given site.

This "application-specific" approach has several benefits over the more generic approaches to site amplification considered previously. The main benefit is that a greater quantity of geotechnical information is integrated into the analysis, which

may better represent an engineering based approach. Whilst a greater computational effort is required to develop the amplification factors, they remain characteristic for the region in question. Implementation of the site amplification within the stochastic earthquake hazard simulation is a relatively simple and computationally efficient procedure.

3.4.2 Liquefaction

The estimation of permanent ground displacement due to liquefaction is adapted largely from the methodology introduced in HAZUS (NIBS 2004). Within this methodology, estimation of the probability of liquefaction is based on the analysis of Youd and Perkins (1978), who introduced classes of liquefaction susceptibility. These classes (Very High, High, Moderate, Low, Very Low and None) are categorised on the basis of deposit type, age and general distribution of cohesionless sediments. Each liquefaction susceptibility category has an associated conditional probability of liquefaction for a given PGA, and a proportion of map unit susceptible to liquefaction. This latter is intended to take into account the variability of soil properties within any given sedimentary class, which may act to inhibit liquefaction at a site.

This formulation may be the simplest approach, requiring only the susceptibility class (which can be inferred from surficial geology), PGA (the peak horizontal ground acceleration, in units of g, at the ground surface), magnitude and depth to the groundwater. Derivation of the probabilities of liquefaction given an input PGA, and the values for the proportions of susceptible map unit for each susceptibility category, can be found in NIBS (2004), as well as the categorisation scheme for liquefaction susceptibility.

The primary advantage of the current methodology is the simplicity and the dependence on few site-specific factors. It may be considered only a first order estimate on the amount of displacement associated with lateral spreading at a site. It may be considered, however, only a first-order estimate on the amount of displacement associated with lateral spreading at a site. Alternative models describing both the probability of liquefaction and the resulting permanent ground deformation could be supported in future.

Despite being a commonly observed liquefaction phenomenon, there are fewer established models that are used in assessment of ground settlement. It has been suggested by Tokimatsu and Seed (1987) that the extent of settlement shows little dependence on the strength of ground motion. This makes characterisation in a hazard framework substantially more challenging. In the present methodology a characteristic settlement is attributed to each susceptibility class, thus making the expected settlement a product of the liquefaction probability and the characteristic settlement.

3.4.3 Slope Displacement

As with the estimators of liquefaction induced displacement, the methodology adopted for estimation of slope displacement is also adopts the landsliding susceptibility classification defined within HAZUS (NIBS 2004). The landsliding susceptibility class is assigned on the basis of geology, slope angle and the position of groundwater with respect to the level of sliding (essentially a wet/dry distinction). For each susceptibility class, a critical acceleration is defined; hence, if PGA exceeds the critical acceleration then displacement is possible. As for the case of liquefaction, each susceptibility category is associated with a percentage of map area having a landslide-susceptible deposit. In the SYNER-G implementation, these factors are implemented as probabilities of observing landsliding at a site, given PGA at the site exceeds the critical acceleration defined for site.

The simplicity of the characterisation of landslide susceptibility is a key advantage of the current approach. The crucial parameter needed for estimation of slope displacement is critical acceleration, or "yield coefficient" (k_y), which corresponds to the threshold acceleration above which slope displacement is initiated. This may be estimated via many different ways, taking into consideration the properties of the slope. The yield coefficient may be specified by the user a priori, or assigned according to the defined susceptibility classes (NIBS 2004).

As with the case of liquefaction, alternative empirical models exist that may better constrain the uncertainty in the slope displacement, whilst retaining practicality for use with common intensity measures. For this purpose the scalar empirical slope displacement model of Saygill and Rathje (2008) is adopted to define the slope displacement as a function of PGA:

$$\ln(PGD) = 5.52 - 4.43\left(\frac{k_y}{PGA}\right) - 20.39\left(\frac{k_y}{PGA}\right)^2 + 42.61\left(\frac{k_y}{PGA}\right)^3 - 28.74\left(\frac{k_y}{PGA}\right)^4 + 0.72\ln(PGA) + \sigma_{\ln PGD} \tag{3.15}$$

where PGD is the sliding displacement in cm, and the total variability described by a Gaussian distribution with zero mean and standard deviation $\sigma_{\ln D}$ of 1.13. Alternative empirical models of slope displacement could be implemented within the same framework, if preferred.

3.4.4 Transient Strain

Transient strain ϵ_S is rarely treated explicitly in analyses of seismic risk to infrastructural systems, as fragility curves for strain-sensitive elements are usually given as functions of peak ground velocity (PGV). For application within the Shakefield

approach, it is more convenient to characterise peak transient ground strain via an empirical model relating the strain to other parameters of ground motion. Using observed ground motions from selected Californian, New Zealand and Japan earthquakes, simple empirical models relating maximum in-plane horizontal strain to PGV (m s^{-1}) or PGA (m s^{-2}) have been determined by Paolucci and Smerzini (2008):

$$\log_{10}\left(\max\left(\epsilon_S\right)\right) = 0.95\log_{10}\left(PGV\right) - 3.07 + \sigma_{\epsilon_s} \tag{3.16}$$

$$\log_{10}\left(\max\left(\epsilon_S\right)\right) = 6.0 \times 10^{-5} PGA + \sigma_{\epsilon_s} \tag{3.17}$$

In both cases the standard deviation (σ_{ϵ_s}) is approximately 0.16.

3.4.5 Coseismic Rupture

Since the development of the original HAZUS methodology several studies have been undertaken that outline a Probabilistic Fault Displacement Hazard Assessment (PFDHA) methodology (Youngs et al. 2003; Petersen et al. 2011; Chen and Petersen 2011; Moss and Ross 2011). The methodology describes the hazard integral as follows Youngs et al. (2003):

$$v_k\left(d\right) = \sum_n \alpha_n\left(m^0\right) \int_{m_0}^{m_u} f_n\left(m\right) \times \left[\int_{r_{min}}^{r_{max}} f_{kn}\left(r|m\right) P_{kn}\left(slip|m,r\right) P_{kn}\left(D > d\,|m,r,slip\right) dr\right] dm \tag{3.18}$$

where $\alpha_n\left(m^0\right)$ is the rate of events in source n with $m \geq m_0$, $f_n\left(m\right)$ the probability density function of the earthquake magnitude (m) for the source n, $f_{kn}\left(r|m\right)$ the conditional probability density function for distance, r, from site k to an earthquake of magnitude m occurring on source n; $P_{kn}\left(slip|m,r\right)$ the probability of observing displacement at a site, given the magnitude and distance, and $P_{kn}\left(D > d\,|m,r,slip\right)$ the probability of exceeding a displacement level d, given that slip is observed at the site. The formulation is adapted slightly for distributed slip on smaller structures away from the principal fault, which need not necessarily be conditional upon the occurrence of slip at the surface from the principal fault but assumes slip at depth. The objective of the rupture object designed here is to attempt to adapt aspects of this formulation, using a stochastic approach to model the conditional probabilities outlined previously.

To implement this approach within a stochastic framework, the process probabilities are broken down into separate steps. The manner in which a stochastically generated fault rupture is distributed across a surface (described in more detail in Sect. 3.5) is already using the seismogenic sources to produce a set of rupture

realisations sufficient to sample $P_{kn}\left(slip|m,r\right)$, the probability of observing slip on the principal fault. At the nodes of the mesh where slip is given to occur, the expected slip is sampled as a ratio of the average displacement on a fault (itself sampled from the magnitude scaling relation of Wells and Coppersmith (1994)), described by a gamma distribution with the cumulative distribution function $F\left(D/AD\right)$. The cumulative distribution function is then sampled using the empirical principal slip models from Youngs et al. (2003), Petersen et al. (2011), and Moss and Ross (2011), for normal faulting, strike-slip faulting or reverse faulting respectively.

Youngs et al. (2003) For normal faulting, the expected slip at a point on the fault is sampled from the CDF of the gamma distribution:

$$F\left(D/AD\right) = \frac{1}{\Gamma\left(a\right)} \int_0^{(D/AD)/b} e^{-t} t^{a-1} dt \tag{3.19}$$

where D/AD is the displacement as a proportion of average displacement, $\Gamma\left(.\right)$ is the gamma function, $a = \exp\left(-0.193 + 1.628\, l/L\right)$ and $b = \exp\left(0.009 - 0.257\, l/L\right)$, where l/L is the ratio of the length from site to the nearest end of the fault, with respect to the total length of the fault. This value is therefore constrained within the range $0 \leq l/L \leq 0.5$

Petersen et al. (2011) Three different functional forms are presented to describe the scaling of D/AD with respect to l/L for strike slip faulting

- Bilinear:

$$\log\left(D/AD\right) = \begin{cases} 8.2525\left(l/L\right) - 2.3010 \pm 1.2962\epsilon_{\log(D/AD)} & \text{for} l/L < 0.3008 \\ 0.1816 \pm 1.0013\sigma_{\log(D/AD)} & \text{for} l/L \geq 0.3008 \end{cases} \tag{3.20}$$

- Quadratic:

$$\begin{aligned} \log\left(D/AD\right) = {} & 14.2824\left(l/L\right) - 19.8833\left(l/L\right)^2 \\ & - 2.6279 \pm 1.1419\sigma_{\log(D/AD)} \end{aligned} \tag{3.21}$$

- Elliptical:

$$\begin{aligned} \log\left(D/AD\right) = {} & 3.2699\sqrt{1 - \frac{1}{0.5^2}\left[\left(l/L\right) - 0.5\right]^2} \\ & - 3.2749 \pm 1.1419\sigma_{\log(D/AD)} \end{aligned} \tag{3.22}$$

The choice of models may be a decision for the user, although the bilinear model is shown to have the lowest aleatory variability.

Moss and Ross (2011) For reverse faults, the displacement as a ratio of average displacement is again assumed to be gamma distributed assuming the same functional form as (3.19), with the shape parameter (a) and scale parameter (b) described by

$$a = \exp\left(-30.4\,(l/L)^3 + 19.9\,(l/L)^2 - 2.29\,(l/L) + 0.574\right) \tag{3.23}$$

$$b = \exp\left(50.3\,(l/L)^3 - 34.6\,(l/L)^2 + 6.6\,(l/L) - 1.05\right) \tag{3.24}$$

Other probability density functions are presented by Moss and Ross (2011); however, the gamma distribution is chosen here for consistency with the Youngs et al. (2003) model for normal faulting.

In addition to the empirical models of slip on the principal rupture, both Youngs et al. (2003) and Petersen et al. (2011) describe empirical models displacement for sites distributed around the rupture. A similar process is followed to that of the on-fault rupture, albeit the empirical models for $P_{kn}\,(slip|m, r)$ and $P_{kn}\,(D > d\,|m, r, slip)$ are sampled directly from the corresponding models for normal faults and strike-slip faults found in Youngs et al. (2003) (Eq. 7 and Appendix A of the original paper) and Petersen et al. (2011) (Eqs. 19 and 20 of the original paper) respectively.

This stochastic implementation of a probabilistic fault displacement hazard process contains many critical developments when compared to previous approaches. The most significant is the inclusion of aleatory uncertainty into the process, something that has been difficult to constrain until this point. The inclusion of distributed (off-fault) rupture is also important in validation studies, where many displacements may be observed without necessarily requiring that the primary rupture propagate to the surface (a circumstance that is more common in the extensional environments of central Italy and Greece). Furthermore, by utilising the same "simplified" rupture propagation process for the purpose of defining both the finite rupture surface for the ground motion attenuation and for the slip displacement, this methodology introduces a consistency in the transient shaking and permanent displacement generation process that is not possible via traditional means of probabilistic shaking hazard and fault displacement hazard analysis alone.

There remain limitations to this approach, however, and these mostly arise from the relative paucity of observational data, particularly in extensional faulting environments. It can be seen in the analysis of Youngs et al. (2003) that empirical models of slip probabilities and displacements are derived from a relatively small database of normal faults, to which European extensional ruptures contribute little.

3.5 Implementation of the Probabilistic Seismic Hazard Methodology

3.5.1 The Stochastic Methodology

The Shakefield procedure outlined in Sect. 3.1 represents a common methodology that can be applied to generate ground motion fields from potential scenario events. The use of Monte Carlo based random simulations of seismicity is also extensible to probabilistic seismic hazard analysis (e.g. Musson 2000; Weatherill and Burton 2010). For the purposes of the SYNER-G project, a general methodology was developed that allows for either to be considered. The following section elaborates upon the general hazard methodology that is used to generate seismic hazard input for multi-system analysis of seismic risk, implemented within the Object-Oriented Framework for Infrastructure Modelling and Simulation (OOFIMS) software described in this book.

One of the most important considerations in the development of a general methodology is the adaptability to different degrees of data information and quality, depending on the case study in question. A multi-tiered approach, particularly with respect to the characterisation of the site and the geotechnical hazard, is necessary in order to allow for application to larger regions. The characterisation of the seismic source and the ground motion attenuation is consistent with that required for regional scale probabilistic seismic hazard analysis. When taking into consideration spatial correlation and cross-correlation between different intensity measures, further adaptability is also necessary.

The general process for a stochastic implementation of a seismic hazard and geotechnical hazard calculator is outlined in Fig. 3.5 (for the general methodology) and Fig. 3.6 for the geotechnical extension. For each iteration the occurrence and corresponding magnitude of the event in each source is sampled from the magnitude frequency distribution of the source. In most of the sources considered in the European case studies this may correspond to the classic double-truncated exponential distribution, but other forms of the distribution can be equally well supported, and of course the same process can be applied to scenario earthquake ruptures.

3.5.1.1 Generation of the Earthquake Rupture

The use of seismogenic fault sources presents a challenge in understanding how to stochastically distribute ruptures across the fault surface in a manner that is consistent with both the properties of the rupture and of the magnitude frequency distribution. For this purpose an iterative procedure is invoked, in which a rupture is initiated from a randomly sampled point in the mesh of the surface (see Fig. 3.7). An automata-style approach is then used in which the rupture expands to the

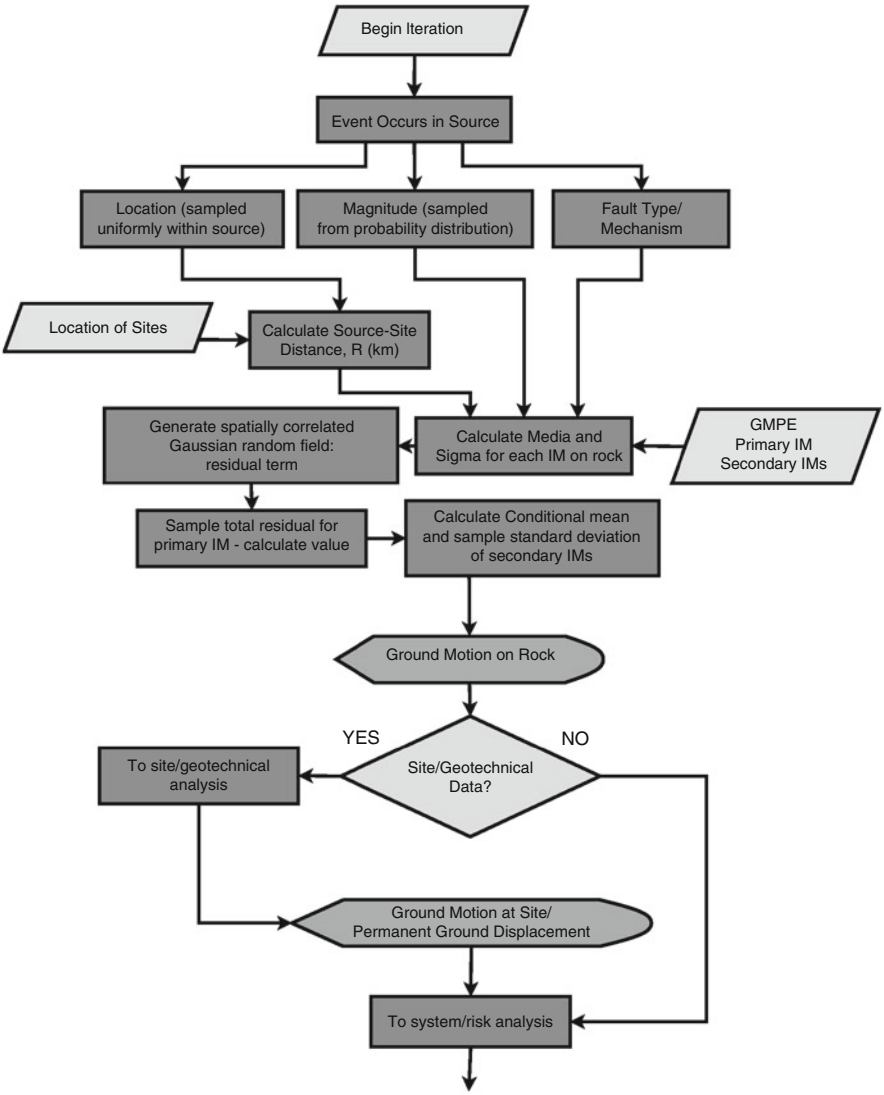

Fig. 3.5 Overview of stochastic seismic hazard simulation procedure. Input (*trapezium*), processes (*rectangle*), decisions (*triangle*) and outputs (*display*)

neighbouring points of an "active" cell on each subsequent iteration, until the total area of the rupture matches the expected area of the rupture for that magnitude. The expected area is sampled from a magnitude scaling relation, such as Wells and Coppersmith (1994) in this case. Rupture expansion is isotropic until it reaches the confining boundaries of the fault surface, at which point it will continue to propagate in the unconfined direction. In principal, certain behaviours of the kinematic rupture

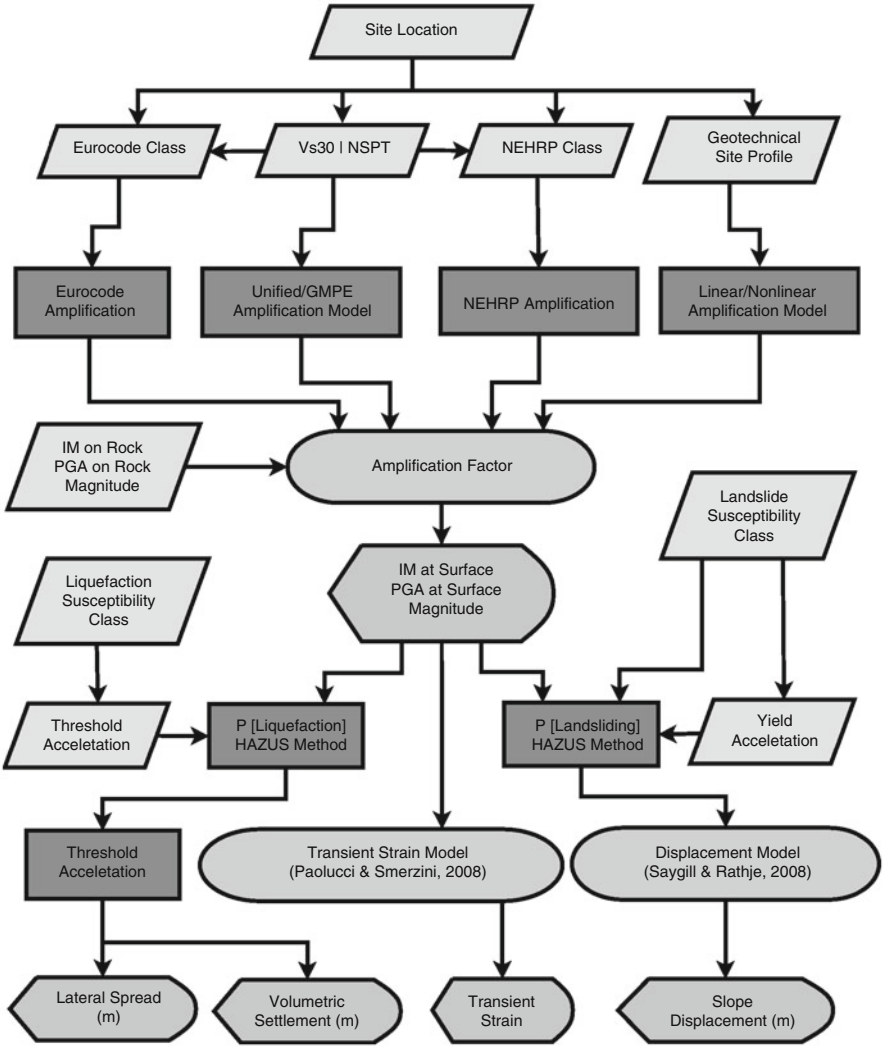

Fig. 3.6 Overview of the process to define the site amplification and geotechnical hazard. Input (*trapezium*), processes (*rectangle*), models (*spheroid*) and outputs (*display*)

process can be mimicked (e.g. unilateral propagation, temporary asperities, down-dip or along-strike dependent hypocentre probability distributions etc.) without necessarily incurring a significant computational cost.

The rupture generated on each simulation can be utilised in two sections of the calculation. The first is for defining the finite surface within the seismogenic fault, from which the finite-distance metrics of the ground motion prediction equation can be determined. The second case is in sampling, in a physically consistent manner,

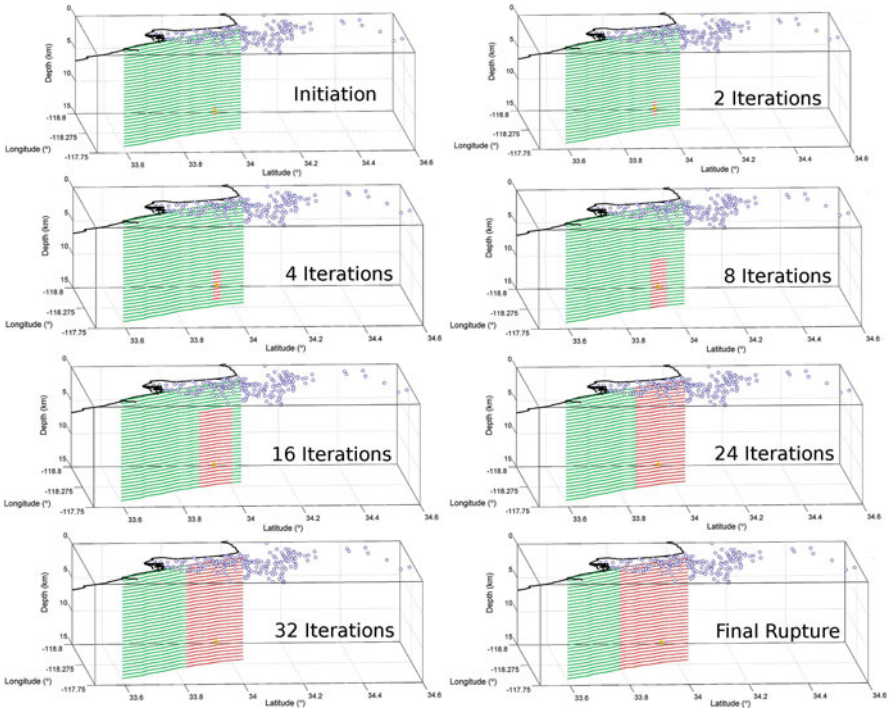

Fig. 3.7 Simple simulation process for the stochastic generation of ruptures (*red*) on a fault surface (*green*). Vertical scale exaggerated

the probability of observing displacement at the ground surface due to on-rupture slip, given a magnitude and distance to the fault rupture. For analysis of seismic risk to lifeline structures such as pipes, rails and tunnels, which require PGD as an input to the fragility functions, this information is relevant.

3.5.2 Issues Emerging in Practice

The general framework presented here for generating stochastic fields of ground motion and permanent ground displacement may still represent an idealised process, only fully applicable in areas where a considerable quantity of input data can be constrained. Arguably the most significant limiting factor in practice, particularly with respect to the geotechnical calculators, is the inability to describe the site conditions and/or source geometries with sufficient accuracy to apply the empirical models of ground motion or displacement across a regional scale, in a manner that is consistent with their derivation. It is therefore inevitable that simplifications will emerge.

Rather than exhaustively list all the possible areas in which uncertainty may be overestimated, underestimated or not even characterised, we shall focus on a few critical areas:

3.5.2.1 Earthquake Source Geometry

Whilst many of the major active fault systems in Europe are well known to geologists, the precise extent of the fault geometries are rarely well constrained. In many parts of the continent, regions of active seismicity still cannot be represented by the fault source typology described previously. Instead, distributed seismicity sources, such as uniform zones of seismicity, are used. In these regions, many state-of-the-art hazard calculators will generate synthetic finite pseudo-ruptures, with properties that are consistent with the seismotectonics of the region in question. Where such sources are invoked, it is certainly the case that rupture displacement calculators, such as the one described here, cannot be utilised.

3.5.2.2 Ground Motion Uncertainty and Correlation

The requirement to consider both the spatial correlation in ground motion and the cross-correlation between different IMs, is both a novel development and a critical requirement of multi-system analyses such as those undertaken within this project. The conditional simulation methodology is an efficient process for generating multiple ground motion fields potentially preserving some of the cross-correlation between IMs, depending on the applicability of the hypotheses of the method. This is not merely a trivial benefit, as the systemic vulnerability algorithms to which these fields are fed do, themselves require considerable computational resources. Both the choice of ground motion model and correlation model will influence the resulting loss analyses. The selection of GMPEs is a common process in seismic hazard analysis, and it could be argued that the consistency of correlation models between European records (Esposito and Iervolino 2011, 2012) and other models in active shallow zones (Jayaram and Baker 2009) would suggest that there is not a strong regionalisation of correlation models within active shallow tectonic regimes.

For the selection of GMPEs for use in the Shakefield process, it is preferable to consider those GMPEs for which PGA, PGV and $S_a\,(T)$ are defined, and form the reference ground motion model for the derivation of the spatial correlation models from European records (Sect. 3.2). For the applications within the SYNER-G project Akkar and Bommer (2010) and Bindi et al. (2010a) GMPEs are preferred.

3.5.2.3 Probabilities of Landsliding/Liquefaction

As described previously, the models for characterising the respective probabilities of liquefaction and landsliding were adopted from those of HAZUS (NIBS 2004). Without further investigation, and validation studies such as the ones undertaken for L'Aquila, Thessaloniki and Vienna within the SYNER-G project, it remains

to be seen to what extent the current methodology for defining liquefaction and landsliding probabilities can be adopted in European terrains, without the need for modification.

3.5.2.4 Geotechnical Site Characterisation Across an Urban Region

One of the principal factors limiting the application of site specific analysis methodologies to urban and regional scales is the paucity of geotechnical data over wider spatial scales, and the challenge of microzoning geotechnical properties given a limited set of samples. This is, of course, dependent on the case study in question. Nevertheless, it can be seen, even in detailed case studies, that in order to include geotechnical effects on an urban scale there is a need to simplify the characterisation of the sites in terms of simpler, yet representative, soil classes and geotechnical failure susceptibility categories. The simplification naturally drives the methodology to seek out those models that may be most broadly applicable in a practical sense. This may include the use of V_{S30}, or similar approaches such as Pitilakis et al. (2013) in favour of a more localised site amplification function, and equally common the use of a generalised design code amplification function based on site category where it is not possible to adequately constrain V_{S30} or equivalent parameter.

3.6 Future Developments in Seismic Hazard Methodologies for Analysis of Seismic Risk to Multi-system Infrastructures

The analysis of seismic risk to multi-system infrastructures presents many new challenges in the characterisation of the ground motion input. Given the inter-connected nature of the different spatial systems, and the heterogeneity of the vulnerable elements within each, it is clearly necessary to implement a procedure for characterising the ground motion fields across many spectral periods, all whilst preserving the correlation structure of the motion.

It is of course recognised that, in terms of correlation, improved results could be achieved for a scenario rupture using numerical simulations of ground motion with a 3D wave propagation model. Whilst these sorts of simulations may be desirable in many situations, their application remains limited when considering the a wide range of stochastic events, each with considerable uncertainty on the physical characteristics of the rupture. This is in large part due to the computational cost of the process, which severely restricts the range of rupture scenarios that can be incorporated into analyses such as these, and the specificity of the physical models of the geological morphology of a region, which limits the applicability over many areas in Europe. However, the use of ground motion simulations for urban scale analysis of risk to urban infrastructure retains great potential for use in future applications. Furthermore, many of the stochastic processes developed within the present methodology can be readily integrated into a simulation-based methodology.

The extension of the seismic hazard modelling process to provide realisations of permanent ground deformation has highlighted the need to develop more empirical models that can be applied over urban and regional scales. There have been many developments in the field of probabilistic liquefaction hazard analysis (e.g., Kramer and Mayfield 2007; Goda et al. 2011), probabilistic seismic sliding displacement hazard (e.g., Rathje and Saygill 2011) and co-seismic rupture displacement hazard (e.g., Youngs et al. 2003; Chen and Petersen 2011). In many of these examples, however, the applications are largely limited to a site-specific context. Despite the limitations in the geotechnical characterisation, empirical methodologies are emerging for characterising soil properties over spatial scales, conditional upon a limited set of observations (Baker and Faber 2008; Chen et al. 2012). These models, and subsequent developments, may assist in increasing the applicability of more site-specific geotechnical hazard analysis procedures to broader scales.

The multi-system infrastructure analyses undertaken within the SYNER-G project illustrate why it is of great benefit, to both the research community and to the end-users of the products, to begin to consolidate existing data (both pre- and post-event). It is difficult to establish the portability of these methodologies to different regions of the globe, without being able to ascertain how microzonation and geotechnical information is represented across different urban regions. The establishment of a unified taxonomy for representing geotechnical data would be a significant step in this direction, both as a means of consolidating a wide and disparate assortment of geotechnical parameters and as a means of establishing a truly hierarchical methodology for undertaking geotechnical seismic hazard assessment in different regions of the globe. This may also be true for many other elements of the systems considered in the infrastructure analysis.

The application of the Shakefield and geotechnical procedure in the case studies described in later chapters will demonstrate the challenges in implementing this approach in a real-world context. It will be shown that the incorporation of the hazard uncertainties and the correlations have a significant impact on the variability of the expected losses, both from single events and from full probabilistic approaches. The need for model evaluation and validation studies is paramount in establishing where improvements to the methodology will be needed, and where the uncertainties may have the greatest impact. Likewise, it is anticipated that future extensions of these applications to different cities both in Europe and across the globe will create many new challenges in implementation.

References

Akkar S, Bommer JJ (2010) Empirical equations for the prediction of PGA, PGV, and spectral accelerations in Europe, the Mediterranean Region, and the Middle East. Seismol Res Lett 81(2):195–206

Baker JW (2007) Correlation of ground motion intensity parameters used for predicting structural and geotechnical response. In: Kanda J, Takada T, Furuta H (eds) Applications of statistics and probability in civil engineering. Taylor & Francis, London/New York

Baker JW, Cornell CA (2006) Correlation of response spectral values for multicomponents of ground motion. Bull Seismol Soc Am 96(1):215–227
Baker JW, Faber MH (2008) Liquefaction risk assessment using geostatistics to account for soil spatial variability. J Geotech Geoenviron Eng 134(1):14–23
Baker JW, Jayaram N (2008) Correlation of spectral acceleration values from NGA ground motion models. Earthq Spectra 24(1):299–317
Bazzurro P, Cornell CA (2004a) Ground-motion amplificationin nonlinear soil sites with uncertain properties. Bull Seismol Soc Am 94(6):2090–2109
Bazzurro P, Cornell CA (2004b) Nonlinear soil-site effects in probabilistic seismic hazard analysis. Bull Seismol Soc Am 94(6):2110–2123
Bindi D, Luzi L, Massa M, Pacor F (2010a) Horizontal and vertical ground motion prediction equations derived from the Italian Accelerometric Archive (ITACA). Bull Earthq Eng 8:1209–1230
Bindi D, Luzi L, Rovelli A (2010b) Ground motion prediction equations GMPEs derived from ITACA. Technical report, Deliverable No. 14, Project S4: Italian Strong Motion Data Base
Bindi D, Pacor F, Luzi L, Puglia R, Massa M, Ameri G, Paolucci R (2011) Ground motion prediction equations derived from the Italian strong ground motion database. Bull Earthq Eng 9:1899–1920
Boore DM, Gibbs JF, Joyner WB, Tinsley JC, Ponti DJ (2003) Estimated ground motion from the 1994 Northridge, California, earthquake at the site of the Iinterstate I-10 and La Cienega Boulevard bridge colapse, West Los Angeles, California. Bull Seismol Soc Am 93(6):2737–2751
Bradley BA (2011a) Correlation of significant duration with amplitude and cumulative intensity measures and its use in ground motion selection. J Earthq Eng 15(6):809–832
Bradley BA (2011b) Empirical correlation of PGA, spectral accelerations and spectrum intensities from active shallow crustal earthquakes. Earthq Eng Struct Dyn 40(15):1707–1721
Chen R, Petersen MD (2011) Probabilistic fault displacement hazards for the Southern San Andreas fault using scenarios and empirical slips. Earthq Spectra 27(2):293–313
Chen Q, Seifried A, Andrade JE, Baker JW (2012) Characterization of random fields and their impact on the mechanics of geosystems at multiple scales. Int J Numer Anal Methods Geomech 36:140–165
Choi Y, Stewart JP (2005) Nonlinear site amplification function of 30m shear wave velocity. Earthq Spectra 21(1):1–30
Crowley H, Bommer JJ, Stafford PJ (2008a) Recent developments in the treatment of ground-motion variability in earthquake loss models. J Earthq Eng 12(S2):71–80
Crowley H, Stafford PJ, Bommer JJ (2008b) Can earthquake loss models be validated using field observations? J Earthq Eng 127:1078–1104
Davis M (1987) Production of conditional simulation via the LU decomposition of the covariance matrix. Math Geol 192:91–98
Esposito S, Iervolino I (2011) PGA and PGV spatial correlation models based on European multievent datasets. Bull Seismol Soc Am 101(5):2532–2541
Esposito S, Iervolino I (2012) Spatial correlation of spectral acceleration in European data. Bull Seismol Soc Am 102(6):2781–2788
FEMA-450 (2003) NEHRP recommended provisions for seismic regulations for new buildings and other structures. Technical report, Federal Emergency Management Agency (FEMA), Washingon, DC
Goda K, Atkinson GM (2009) Probabilistic characterisation of spatial correlated response spectra for earthquakes in Japan. Bull Seismol Soc Am 99(5):3003–3020
Goda K, Atkinson GM (2010) Intraevent spatial correlation of ground motion parameters using SK-net data. Bull Seismol Soc Am 100(6):3055–3067
Goda K, Hong HP (2008a) Spatial correlation of peak ground motions and response spectra. Bull Seismol Soc Am 98(1):354–365
Goda K, Hong HP (2008b) Estimation of seismic loss for spatially distributed buildings. Earthq Spectra 24(4):889–910

Goda K, Atkinson GM, Hunter JA, Crow H, Motazedian D (2011) Probabilistic liquefaction hazard analysis for four Canadian cities. Bull Seismol Soc Am 101(1):190–201

Hong HP, Zhang Y, Goda K (2009) Effect of spatial correlation on estimated ground motion prediction equations. Bull Seismol Soc Am 99(2A):928–934

Iervolino I, Giorgio M, Galasso C, Manfredi G (2010) Conditional hazard maps for secondary intensity measures. Bull Seismol Soc Am 100(6):3312–3319

Inoue T, Cornell CA (1990) Seismic hazard analysis of multi-degree-of-freedom structures. Technical report, RMS, Stanford

Jayaram N, Baker JW (2008) Statistical tests of the joint distribution of spectral acceleration values. Bull Seismol Soc Am 98(5):2231–2243

Jayaram N, Baker JW (2009) Correlation model of spatially distributed ground motion intensities. Earthq Eng Struct Dyn 38:1687–1708

Jayaram N, Baker JW (2010a) Efficient sampling and data reduction techniques for probabilistic seismic lifeline risk assessment. Earthq Eng Struct Dyn 39(10):1109–1131

Jayaram N, Baker JW (2010b) Cequations spatial correlation in mixed-effects regression, and impact on ground motion models. Bull Seismol Soc Am 100(6):3295–3303

Kramer SL, Mayfield RT (2007) Return period of soil liquefaction. J Geotech Geoenviron Eng 133(7):802–813

Loth C, Baker JW (2013) A spatial cross-correlation model of spectral accelerations at multiple periods. Earthq Eng Struct Dyn 42:397–417

Moss RES, Ross ZE (2011) Probabilistic fault displacement hazard analysis for reverse faults. Bull Seismol Soc Am 101(4):1542–1553

Musson R (2000) The use of Monte Carlo simulations for seismic hazard assessment in the UK. Annali di Geofisica 43(1):1–9

NIBS N (2004) HAZUS-MH: techincal manual. Technical report, Federal Emergency Management Agency (FEMA), Washington, DC

Oliver DS (2003) Gaussian cosimulation: modelling of the cross-covariance. Math Geol 356:681–698

Paolucci R, Smerzini C (2008) Earthquake-induced transient ground strains from dense seismic networks. Earthq Spectra 24(2):453–470

Park J, Bazzurro P, Baker JW (2007) Modeling spatial correlation of ground motion intensity measures for regional seismic hazard and portfolio loss estimation. In: Kanda J, Takada T, Furuta H (eds) Applications of statistics and probability in civil engineering. Taylor & Francis, London

Petersen MD, Dawson TE, Chen R, Cao T, Wills CJ, Schwartz DP, Frankel AD (2011) Fault displacement hazard for strike-slip faults. Bull Seismol Soc Am 101(2):805–825

Pitilakis K, Riga E, Anastasiadis A (2012) Design spectra and amplification factors for Eurocode 8. Bull Earthq Eng 10:1377–1400

Pitilakis K, Riga E, Anastasiadis A (2013) New code site classification, amplification factors and normalised response spectra based on a worldwide ground-motion database. Bull Earthq Eng 11(4):925–966

Rathje EM, Saygill G (2011) Estimating fully probabilistic seismic sliding displacements of slopes from a pseudoprobabilistic approach. J Geotech Geoenviron Eng 137(3):208–217

Robinson D, Dhu T, Schneider J (2006) SUA: a compter program to compute site-response and epistemc ununcertainty for probabilistic seismic hazard analysis. Comput Geosci 32:109–123

Saygill G, Rathje EM (2008) Empirical predictive models for earthquake-induced sliding displacements of slopes. J Geotech Geoenviron Eng 134(6):790–803

Sokolov V, Wenzel F, Jean WY, Wen KL (2010) Uncertainty and spatial correlation of earthquake ground motion in Taiwan. Terr Atmos Ocean Sci 21(6):905–921

Tokimatsu K, Seed HB (1987) Evaluation of settlement in sands due to earthquake shaking. J Geotech Geoenviron Eng 113(8):861–878

Wang M, Takada T (2005) Macrospatial correlation model of seismic ground motions. Earthq Spectra 21:1137–1156

Weatherill G, Burton PW (2010) An alternative approach to probabilistic seismic hazard analysis in the Aegean region using Monte Carlo simulation. Tectonophysics 492:253–278

Wells DL, Coppersmith KJ (1994) New empirical relationships among magnitude, rupture length, rupture width, rupture area, and surface displacement. Bull Seismol Soc Am 84(4):974–1002

Youd TL, Perkins DM (1978) Mapping of liquefaction induced ground failure potential. J Geotech Eng Div ASCE 1044:433–466

Youngs RR, Arabasz WJ, Ernest Anderson R, Ramelli AR, Aki JP, Slemmons DB, McCalpin JP, Doser DI, Fridrich CJ, Swan FH III, Rogers AM, Yount JC, Anderson LW, Smith KD, Bruhn RL, Knuepfer PLK, Smith RB, dePolo CM, O'Leary DW, Coppersmith KJ, Pezzopane SK, Schwartz DP, Whitney JW, Olig SS, Toro GR (2003) A methodology for probabilistic fault displacement hazard analysis (PFDHA). Earthq Spectra 19(1):191–219